Spectral weight suppression near a metal-insulator transition in a double-layer electron-doped iridate

Gregory Affeldt, Tom Hogan, Christopher L. Smallwood, Tanmoy Das, Jonathan D. Denlinger, Stephen D. Wilson, Ashvin Vishwanath, and Alessandra Lanzara

Phys. Rev. B **95**, 235151 — Published 28 June 2017

DOI: 10.1103/PhysRevB.95.235151

Spectral Weight Suppression near a Metal-Insulator Transition in a Double Layer Electron-Doped Iridate

Gregory Affeldt,[1,2] Tom Hogan,[3,4] Christopher L. Smallwood,[1,2] Tanmoy Das,[5] Jonathan D. Denlinger,[6] Stephen D. Wilson,[7] Ashvin Vishwanath,[1,2] and Alessandra Lanzara[1,2]

[1]*Materials Sciences Division, Lawrence Berkeley National Laboratory, Berkeley, CA*

[2]*Department of Physics, University of California, Berkeley, CA*

[3]*Department of Physics, Boston College, MA*

[4]*Materials Department, University of California, Santa Barbara, CA*

[5]*Department of Physics, Indian Institute of Science, Bangalore-560012, India*

[6]*Advanced Light Source, Lawrence Berkeley National Laboratory, Berkeley, CA*

[7]*Materials Department, University of California Santa Barbara, Santa Barbara, CA*

(Dated: April 28, 2017)

Abstract

The perovskite iridates Sr_2IrO_4 and $Sr_3Ir_2O_7$ represent novel systems for exploring the electronic structure that is characteristic of Mott insulators upon carrier doping. Using angle-resolved photoemission spectroscopy (ARPES), we reveal a previously unobserved suppression of spectral weight near the Fermi level in the conduction band of very lightly electron-doped $(Sr_{1-x}La_x)_3Ir_2O_7$ followed by a loss of coherence at high temperature. The doping and temperature dependence of this suppression suggests a correspondence with the antiferromagnetic Mott state. These results connect $(Sr_{1-x}La_x)_3Ir_2O_7$ to other doped Mott insulators and add to the growing evidence of universal physics in these systems.

The $j_{\rm eff} = \frac{1}{2}$ Mott state formed in the layered perovskite iridates[1] has presented exciting similarities to the spin-$\frac{1}{2}$ Mott insulators, especially the cuprate superconductors. In particular, ARPES measurements of doped Sr_2IrO_4, in which the low-energy interactions of the spin-orbit coupled moments obey a Heisenberg Hamiltonian equivalent to the cuprates[2], have shown striking similarities to the cuprate pseudogap state[3–6] and even an apparently *d*-wave gap that may be indicative of superconductivity[7]. Less attention has been paid to the more three-dimensional bilayer compound $Sr_3Ir_2O_7$, which has a smaller gap due to stronger *c*-axis coupling and a magnetic state aligned along the *c*-axis [8–12] in contrast to the *ab*-plane magnetization of both Sr_2IrO_4 and the cuprates. Existing ARPES studies on the bulk electron-doped $(Sr_{1-x}La_x)_3Ir_2O_7$ have focused mostly on samples near and above x = 4%, where transport experiments observe a metal-insulator transition[13], and report a correlated metallic state with small electron-like Fermi pockets[14–16]. Here we report a detailed doping and temperature dependent study across the metal-insulator transition (near x = 4%) in $(Sr_{1-x}La_x)_3Ir_2O_7$, from undoped (x = 0%) well into the metallic regime (x = 6%). Samples measured in the antiferromagnetic regime are marked by a low-energy suppression of spectral weight near the chemical potential and an electron-like band at deeper binding energy. With increasing doping, this band moves to lower energy and in the metallic samples this band clearly disperses across the chemical potential. We further observe in all samples a drastic reduction of the coherence of the conduction band at a temperature scale that increases with doping, which may signal another physical transition in this system related to the onset of metallicity.

Single-crystal samples of $(Sr_{1-x}La_x)_3Ir_2O_7$ were synthesized using a flux method as described elsewhere[17]. ARPES measurements were performed at beamlines 4.0.3 and 10.0.1 of the Advanced Light Source at temperatures ranging from 15 K to 240 K. The samples were cleaved *in situ* and measured at pressures better than 6 $\times 10^{-11}$ Torr. The chemical potential was referenced to a polycrystalline gold surface evaporated *in situ* on the sample puck for measurements at beamline 4.0.3 or a separate calibrating gold film sample with identical beamline configuration at ALS beamline 10.0.1.

The first two panels of figure 1 show the lowest energy states for undoped and very lightly (x=1%) doped $(Sr_{1-x}La_x)_3Ir_2O_7$, still within the antiferromagnetic phase [17]. In each, the dashed white square corresponds to the unreconstructed surface Brillouin zone (BZ) which is reduced to the solid square BZ by the staggered rotation of Ir-O octahedra. In the undoped

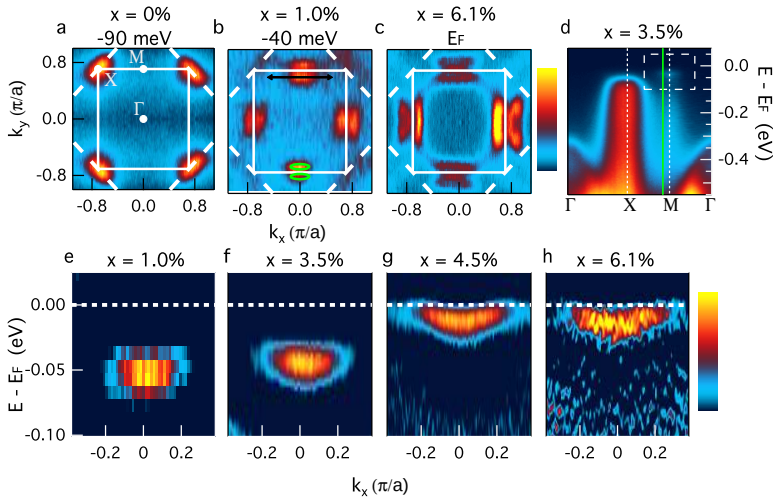

Figure 1. Occupation of the conduction band in $(Sr_{1-x}La_x)_3Ir_2O_7$. (a) ARPES intensity 90 meV below the Fermi surface measured at 15 K in $Sr_3Ir_2O_7$ (x=0%), symmetrized across $k_y = 0$ (b) ARPES intensity 40 meV below the Fermi level measured at 20 K in $(Sr_{0.99}La_{0.01})_3Ir_2O_7$ (x=1% sample). Overlaid green contours are the theoretical Fermi surface, calculated using LDA+SOC+U for this sample. (c) ARPES intensity at the Fermi energy in an x = 6% sample at 20 K, symmetrized across $k_y = 0$. (d) Raw ARPES spectrum along high symmetry directions in the first Brillouin zone of a sample with x = 3.5%. (e) Second energy derivative of ARPES intensity near the Fermi level along the conduction band pocket (indicated by the black arrow in panel b and dashed box in panel e). (f)-(h): the same as panel e for samples with doping levels x=3.5%, 4.5%, and 6%

sample, we observe the valence band maxima at the X point at 90 meV below E_F, in rough agreement with previous ARPES studies[18–22]. With even 1% doping, small pockets appear near the M point. In line with previous ARPES studies of doped $(Sr_{1-x}La_x)_3Ir_2O_7$ [15, 16] we identify the band at the M point as the conduction band. Comparison to band structure calculations for undoped $Sr_3Ir_2O_7$ [18] suggest that its origin is the $j_{\text{eff}} = \frac{1}{2}$ upper Hubbard band, though we cannot rule out an in-gap state. The former would be similar to the situation in the hole-doped system $Sr_2Ir_{1-x}Rh_xO_4$, where there is experimental evidence that doped holes directly occupy the lower Hubbard band [5]. These states are consistent with the predicted elliptical Fermi surface predicted by LDA+SOC+U calculations (shown

by green contours in figure 1b), and their Luttinger volume is consistent with the addition of 0.015 electrons per Ir site. This corresponds to a doping level of x = 1% and is in line with the sample composition as measured by energy-dispersive x-ray scattering. The doping level is similarly determined for each sample measured, as detailed in the Supplemental material [33].

To better visualize the band dispersion, in figure 1e-h we show the second derivative ARPES intensity maps near the M point, along the k-space cut shown in figure 1b (see horizontal black arrow) for samples with dopings of 1%, 3.5%, 4.5%, and 6%. These data clearly show that at very low doping the band does not cross the Fermi level and shows an absence of APRES spectral weight near the chemical potential. This suppression of spectral weight, together with the lack of back bending at E_F and the shape of the symmetrized EDCs (energy distribution curves) resembles the so-called pseudogap feature observed in other correlated materials [23–25]. As the doping increases to 4.5% and 6%, no suppression of spectral weight is observed and the band crosses the chemical potential (see fig 1g,h). While the occupied bandwidth of this conduction band increases with doping as expected, the band bottom moves toward the chemical potential with doping from x = 1% until x = 4.5% as the energy scale of the spectral weight suppression decreases more quickly than the chemical potential shift induced by doping.

In order to investigate the origin of this suppression, we studied its evolution with both temperature and doping across the reported metal-insulator transition. In figure 2, we plot EDCs integrated over a small angular range near k_F ($\pm 0.05^\circ$) along the $\Gamma - M$ direction as a function of doping. For the x = 1% and 3.5%, samples where there is no spectral weight at the chemical potential, we used a momentum corresponding to the MDC peak at the lowest binding energy for which such peaks were distinguishable. Figure 2a shows the low-temperature (15-20 K) EDCs for each doping. Consistent with our observations from the energy-momentum second derivative plots, there is a gap between the leading edge of the EDC and E_F in the x=1% and x=3.5% samples, while the spectral weight crosses the chemical potential in the x=4.5% and x=6% samples. By fitting the leading edge of these integrated EDCs we extract a gap value of 42 meV for the x = 1% sample and of 21 meV for the x = 3.5% sample.

In figure 2b-d we show the temperature dependence of the integrated EDCs for the x = 1% sample. In the low-temperature regime, a relatively sharp quasiparticle peak is present

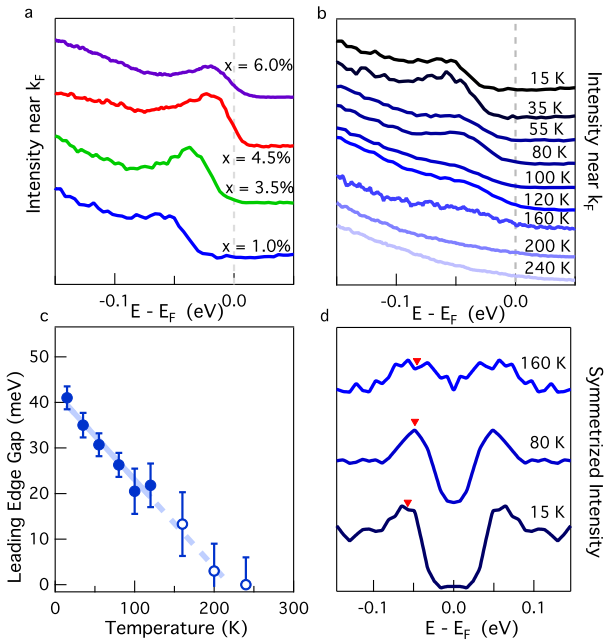

Figure 2. Doping and temperature dependence of the observed spectral weight suppression (a): Energy distribution of spectral weight integrated near k_F at low temperature (15 to 20 K) for each doping level measured (b) Temperature dependence of the same integrated EDCs in an x=1% sample. EDCs are normalized by their value at -150 meV for clarity. (c) Temperature dependence of the leading-edge gap value extracted from integrated EDCs in (b). (d) Symmetrized EDCs for selected temperatures in the x = 1 % sample showing the evolution of the quasiparticle peak position for each temperature. In each, a smooth background fit for -0.15 eV $\leq$ E $\leq$ -0.1 eV was subtracted. Red triangles mark approximate peak positions, determined from the second derivative.

at energies near 50 meV with a narrow leading edge. As the temperature further increases, the leading edge appears to shift closer to the Fermi level, followed by a decrease of the quasiparticle peak. Figure 2c depicts the gap value extracted from this leading edge method for each temperature, which appears to fall off approximately linearly with temperature to a closure around the Neel temperature at 240 K. This method is less reliable at higher temperatures where the peak is less well defined, particularly at and above 160 K, where open symbols and a dashed guide to the eye are used to indicate this uncertainty. An alternative method for examining the temperature dependence of the gap is the use of symmetrized EDCs, like those shown in figure 2d. In the approximation of particle-hole symmetry, this

symmetrization removes the effect of the Fermi-Dirac distribution on the lineshape, which can be of particular importance with small gaps and at higher temperatures. In the 15 K and 80 K data, we can see that the peak corresponding to the conduction band (marked with a red triangle) remains well-defined, with a slight shift and broadening between these two temperatures. A major effect of increasing temperature appears to be the filling of the gap, reminiscent of the pseudogap behavior in cuprate superconductors[26, 27]. The EDCs measured at 200 K and 240 K are nearly featureless when symmetrized, a signature of the gap "filling in" with additional spectral weight near E_F.

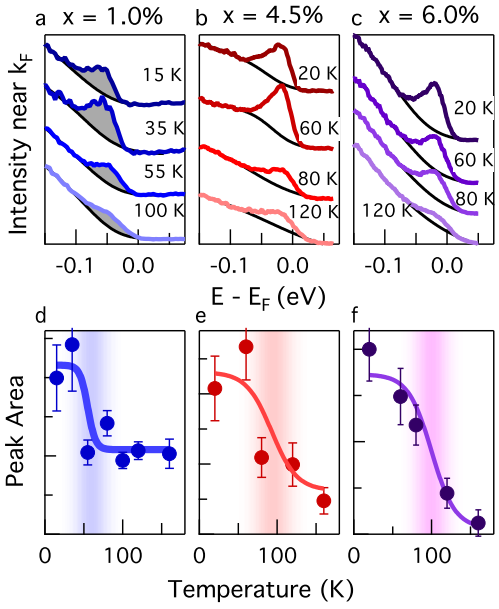

Figure 3. Doping and temperature dependence of coherent peak. (a) - (c) Integrated EDCs at M (as in figure 2) for various temperatures for x = 1%, 4.5%, and 6% samples with background fits (black traces) and extracted peak areas. (d) - (f) Temperature evolution of the background-subtracted peak area for x = 1%, 4.5%, and 6% samples, respectively.

A further examination of the EDCs as a function of temperature reveals another interesting property of these data: the well-defined coherent peak observed at low temperature for the conduction band has a peculiar dependence on temperature and doping. Specifically, the peak area remains constant across the low-temperature region then diminishes rapidly across a narrow temperature range. This evolution of the quasiparticle peak is depicted in figure 3a-c for the x = 1%, 3.5%, and 6% samples. To extract the quasiparticle weight (corresponding to the grey areas in figure 3a) for each EDC, we fit a background function

consisting of a Fermi-Dirac distribution paired with a linear density of states to the energy regions away from the peak (e.g., from -0.2 to -0.1 eV and 0.01 eV to 0.05 eV). Subtracting this background from the integrated EDC isolates the peak, whose integral is taken as a measure of the quasiparticle weight. Figure 3d-f display the evolution of this peak area with respect to temperature for each measured doping. The curves are guides to the eye. We observe a reduction of nearly 50% over a temperature range of approximately 40 K in each of these samples and find that the transition temperature increases monotonically with doping.

This loss of coherence is similar to that previously observed in the related manganite $La_{1.2}Sr_{1.8}Mn_2O_7$ (LSMO). In this system, a coherent quasiparticle is observed near the Fermi level at low temperatures and undergoes a rapid decrease in weight over a narrow temperature range and eventually disappears at the ferromagnetic metal to paramagnetic insulator transition temperature. The low-temperature coherence is attributed to a condensed polaron state[23], though a later work questions this interpretation[28]. This polaron condensation is suggested as a mechanism for the stabilization of the metallic state. Similar physics may be present in the presently-studied compound where both the sharpness of the coherent peak and the coherence loss temperature increase in the metallic regime, suggesting a connection between the low-temperature coherence and the formation of the metallic state. Indeed, polaronic physics have been suggested in undoped $Sr_3Ir_2O_7$ by a recent ARPES study[21] and have been suggested to explain other signatures in layered perovskite iridates [29], including the destruction of the magnetic state at temperatures much smaller than the magnon gap temperature in $Sr_3Ir_2O_7$. Alternatively, the loss of coherence may be related to that observed in the layered cobaltates $(Bi_{0.5}Pb_{0.5})_2Ba_3Co_2O_y$ and $NaCo_2O_4$[24], where such a loss is attributed to a crossover in dimensionality as c-axis transport becomes incoherent. The lower resistivity anisotropy in $Sr_3Ir_2O_7$ relative to the cobaltates, however, suggests that this is an unlikely explanation for the coherence loss as such a transition would likely occur at significantly higher temperature.

To summarize the data, we compare the phase diagram as determined via ARPES to that from a recent scattering, transport, and magnetization study[17] on the same system in figure 4. The doping and temperature dependence of the spectral weight suppression suggests an identification of this feature with the magnetic ordering along (π, π) observed via X-ray scattering[17, 30]. We note also that the drastic change in the gap magnitude over

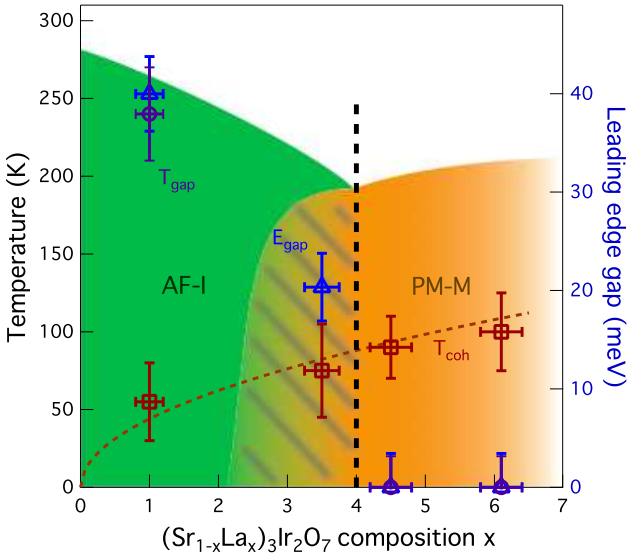

Figure 4. Phase diagram of $(Sr_{1-x}La_x)_3Ir_2O_7$. T_{gap} is the temperature at which the leading edge gap appears to vanish. E_{gap} denotes the leading edge gap magnitude in the lowest temperature measurement. T_{coh} denotes the characteristic temperature associated with the loss in coherent spectral weight as discussed in figure 3. AF-I and PM-M regions are taken from a recent scattering-based study[17]

the short doping range from x = 3.5% to x = 4.5% is consistent with the reported first-order melting of the antiferromagnetic state[17]. The doping dependence of the coherence-loss temperature for the conduction band suggests that it may be connected to the onset of the metallic state with doping. It is unlikely to be connected to the structural transition reported from scattering[17] as the structural transition temperature is significantly higher in the fully metallic samples where both are observed.

This phase diagram highlights several of the ways in which $(Sr_{1-x}La_x)_3Ir_2O_7$ and its spectral weight suppression are similar to other Mott systems, including Sr_2IrO_4. In both cases, a low-doping state marked by the absence of quasiparticles near the chemical potential emerges near the antiferromagnetic Mott state and then vanishes with further doping. While the spectral weight suppression appears to be linked to the antiferromagnetic state in $(Sr_{1-x}La_x)_3Ir_2O_7$, further work is required to identify a microscopic mechanism giving rise to the suppression. No clear identification exists in pseudogapped systems as magnetism, superconductivity, and charge density waves, among other phenomena, provide possible and contested origins of the pseudogap [25, 31]. In fact, the role of magnetism in the cuprate

pseudogap is called into question by a similar gap magnitude in nickelates with much weaker magnetism[32]. The apparent lack of momentum dependence in the spectral weight suppression differs from the highly anisotropic pseudogap, though the smaller size of the Fermi surface limits a full exploration of the momentum dependence.This may be due to different nesting conditions provided by the Fermi surface geometry, as the entire M-point pocket in $(Sr_{1-x}La_x)_3Ir_2O_7$ is nearly nested by a vector near (π, π) while pseudogapped systems are nested only near the antinodal direction. Further, this low-doping state gives way to a metallic region with signatures of another ordering; in $(Sr_{1-x}La_x)_3Ir_2O_7$ this is marked by the coherence loss transition instead of superconductivity. Lastly, we note the different band signatures of the metal-insulator transition: in $(Sr_{1-x}La_x)_3Ir_2O_7$ metallicity is reached when the spectral weight suppression decreases to zero energy leaving small electron-like Fermi surface pockets while in $(Sr_{1-x}La_x)_2IrO_4$ the Mott gap collapses at low doping and a large hole-like Fermi surface emerges [3, 4].

The observation of a low-energy spectral weight suppression in very lightly doped $(Sr_{1-x}La_x)_3Ir_2O_7$ presents an important similarity to other doped Mott insulators and reinforces recent evidence that such features may be universal in these systems. The different characteristics of this suppression relative to the pseudogap observed in Sr_2IrO_4 and the cuprates, along with the apparent absence of superconductivity in $Sr_3Ir_2O_7$, shows the importance of dimensionality in these systems beyond the previously noted differences in magnetic ordering. Further study of these signatures and their relation to each other may provide valuable insights into the role of dimensionality in doped Mott insulators and the necessary ingredients for unconventional superconductivity in these systems.

Acknowledgements

We thank J. Analytis and D.-H. Lee for useful discussions. This work was primarily funded by the U.S. Department of Energy, Office of Science, Office of Basic Energy Sciences, Materials Sciences and Engineering Division under Contract No. DE-AC02-05-CH11231 (Quantum materials KC2202) (G.A.,C.L.S., A.L.). Crystal growth was supported by NSF CAREER Award No. DMR-1056625 (S. D.W.) and DMR-1121053 (T. H.).

[1] B. J. Kim, H. Jin, S. J. Moon, J.-Y. Kim, B.-G. Park, C. S. Leem, J. Yu, T. W. Noh, C. Kim, S.-J. Oh, J.-H. Park, V. Durairaj, G. Cao, and E. Rotenberg, "Novel $J_{\rm eff} = 1/2$ mott state

induced by relativistic spin-orbit coupling in Sr_2IrO_4," *Phys. Rev. Lett.*, vol. 101, p. 076402, Aug 2008.

[2] G. Jackeli and G. Khaliullin, "Mott insulators in the strong spin-orbit coupling limit: From heisenberg to a quantum compass and kitaev models," *Phys. Rev. Lett.*, vol. 102, p. 017205, Jan 2009.

[3] Y. K. Kim, O. Krupin, J. D. Denlinger, A. Bostwick, E. Rotenberg, Q. Zhao, J. F. Mitchell, J. W. Allen, and B. J. Kim, "Fermi arcs in a doped pseudospin-1/2 Heisenberg antiferromagnet," *Science*, vol. 345, no. 6193, pp. 187–190, 2014.

[4] A. de la Torre, S. McKeown Walker, F. Y. Bruno, S. Riccó, Z. Wang, I. Gutierrez Lezama, G. Scheerer, G. Giriat, D. Jaccard, C. Berthod, T. K. Kim, M. Hoesch, E. C. Hunter, R. S. Perry, A. Tamai, and F. Baumberger, "Collapse of the mott gap and emergence of a nodal liquid in lightly doped Sr_2IrO_4," *Phys. Rev. Lett.*, vol. 115, p. 176402, Oct 2015.

[5] Y. Cao, Q. Wang, J. A. Waugh, T. J. Reber, H. Li, X. Zhou, S. Parham, S.-R. Park, N. C. Plumb, E. Rotenberg, A. Bostwick, J. D. Denlinger, T. Qi, M. A. Hermele, G. Cao, and D. S. Dessau, "Hallmarks of the Mott-metal crossover in the hole-doped pseudospin-1/2 Mott insulator Sr_2IrO_4," *Nature Communications*, vol. 7, April 2016.

[6] A. Damascelli, Z. Hussain, and Z.-X. Shen, "Angle-resolved photoemission studies of the cuprate superconductors," *Rev. Mod. Phys.*, vol. 75, pp. 473–541, Apr 2003.

[7] Y. Kim, N. Sung, J. Denlinger, and B. Kim, "Observation of a d-wave gap in electron-doped sr2iro4," *Nature Physics*, vol. 12, no. 1, pp. 37–41, 2016.

[8] I. Nagai, Y. Yoshida, S. I. Ikeda, H. Matsuhata, H. Kito, and M. Kosaka, "Canted antiferromagnetic ground state in $Sr_3Ir_2O_7$," *Journal of Physics: Condensed Matter*, vol. 19, p. 136214, apr 2007.

[9] S. Boseggia, R. Springell, H. C. Walker, a. T. Boothroyd, D. Prabhakaran, S. P. Collins, and D. F. McMorrow, "On the magnetic structure of $Sr_3Ir_2O_7$: an x-ray resonant scattering study.," *Journal of physics. Condensed matter : an Institute of Physics journal*, vol. 24, p. 312202, aug 2012.

[10] C. Dhital, S. Khadka, Z. Yamani, C. de la Cruz, T. Hogan, S. Disseler, M. Pokharel, K. Lukas, W. Tian, C. Opeil, *et al.*, "Spin ordering and electronic texture in the bilayer iridate $Sr_3Ir_2O_7$," *Physical Review B*, vol. 86, no. 10, p. 100401, 2012.

[11] J.-M. Carter and H.-Y. Kee, "Microscopic theory of magnetism in $Sr_3Ir_2O_7$," *Physical Review*

B, vol. 87, p. 014433, jan 2013.

[12] S. Fujiyama, K. Ohashi, H. Ohsumi, K. Sugimoto, T. Takayama, T. Komesu, M. Takata, T. Arima, and H. Takagi, "Weak antiferromagnetism of $J_{\text{eff}} = \frac{1}{2}$ band in bilayer iridate $Sr_3Ir_2O_7$," *Physical Review B*, vol. 86, p. 174414, nov 2012.

[13] L. Li, P. P. Kong, T. F. Qi, C. Q. Jin, S. J. Yuan, L. E. DeLong, P. Schlottmann, and G. Cao, "Tuning the $J_{\text{eff}} = \frac{1}{2}$ insulating state via electron doping and pressure in the double-layered iridate $Sr_3Ir_2O_7$," *Phys. Rev. B*, vol. 87, p. 235127, Jun 2013.

[14] J. He, T. Hogan, T. R. Mion, H. Hafiz, Y. He, J. D. Denlinger, S.-K. Mo, C. Dhital, X. Chen, Q. Lin, Y. Zhang, M. Hashimoto, H. Pan, D. H. Lu, M. Arita, K. Shimada, R. S. Markiewicz, Z. Wang, K. Kempa, M. J. Naughton, A. Bansil, S. D. Wilson, and R.-H. He, "Spectroscopic evidence for negative electronic compressibility in a quasi-three-dimensional spin-orbit correlated metal," *Nat Mater*, vol. 14, pp. 577–582, June 2015.

[15] J. He, H. Hafiz, T. R. Mion, T. Hogan, C. Dhital, X. Chen, Q. Lin, M. Hashimoto, D. H. Lu, Y. Zhang, R. S. Markiewicz, A. Bansil, S. D. Wilson, and R.-H. He, "Fermi Arcs vs. Fermi Pockets in Electron-doped Perovskite Iridates," *Sci. Rep.*, vol. 5, Feb. 2015.

[16] A. de la Torre, E. Hunter, A. Subedi, S. McKeown Walker, A. Tamai, T. Kim, M. Hoesch, R. Perry, A. Georges, and F. Baumberger, "Coherent Quasiparticles with a Small Fermi Surface in Lightly Doped $Sr_3Ir_2O_7$," *Phys. Rev. Lett.*, vol. 113, p. 256402, Dec 2014.

[17] T. Hogan, Z. Yamani, D. Walkup, X. Chen, R. Dally, T. Z. Ward, J. Hill, Z. Islam, V. Madhavan, and S. D. Wilson, "First-order Melting of a Weak Spin-Orbit Mott Insulator into a Correlated Metal," *Phys. Rev. Lett.*, vol. 114, p. 257203, June 2015.

[18] Q. Wang, Y. Cao, J. A. Waugh, S. R. Park, T. F. Qi, O. B. Korneta, G. Cao, and D. S. Dessau, "Dimensionality-controlled Mott transition and correlation effects in single-layer and bilayer perovskite iridates," *Phys. Rev. B*, vol. 87, p. 245109, Jun 2013.

[19] L. Moreschini, S. Moser, A. Ebrahimi, B. Dalla Piazza, K. S. Kim, S. Boseggia, D. F. McMorrow, H. M. Rønnow, J. Chang, D. Prabhakaran, A. T. Boothroyd, E. Rotenberg, A. Bostwick, and M. Grioni, "Bilayer splitting and wave functions symmetry in $Sr_3Ir_2O_7$," *Phys. Rev. B*, vol. 89, p. 201114, May 2014.

[20] B. M. Wojek, M. Berntsen, S. Boseggia, A. Boothroyd, D. Prabhakaran, D. McMorrow, H. Rønnow, J. Chang, and O. Tjernberg, "The $J_{\text{eff}} = \frac{1}{2}$ insulator $Sr_3Ir_2O_7$ studied by means of angle-resolved photoemission spectroscopy," *Journal of Physics: Condensed Matter*, vol. 24,

no. 41, p. 415602, 2012.

[21] P. D. C. King, T. Takayama, A. Tamai, E. Rozbicki, S. M. Walker, M. Shi, L. Patthey, R. G. Moore, D. Lu, K. M. Shen, H. Takagi, and F. Baumberger, "Spectroscopic indications of polaronic behavior of the strong spin-orbit insulator $Sr_3Ir_2O_7$," *Phys. Rev. B*, vol. 87, p. 241106, Jun 2013.

[22] C. Liu, S.-Y. Xu, N. Alidoust, T.-R. Chang, H. Lin, C. Dhital, S. Khadka, M. Neupane, I. Belopolski, G. Landolt, H.-T. Jeng, R. S. Markiewicz, J. H. Dil, A. Bansil, S. D. Wilson, and M. Z. Hasan, "Spin-correlated electronic state on the surface of a spin-orbit mott system," *Phys. Rev. B*, vol. 90, p. 045127, Jul 2014.

[23] N. Mannella, W. L. Yang, K. Tanaka, X. J. Zhou, H. Zheng, J. F. Mitchell, J. Zaanen, T. P. Devereaux, N. Nagaosa, Z. Hussain, and Z.-X. Shen, "Polaron coherence condensation as the mechanism for colossal magnetoresistance in layered manganites," *Phys. Rev. B*, vol. 76, p. 233102, Dec 2007.

[24] T. Valla, P. D. Johnson, Z. Yusof, B. Wells, Q. Li, S. M. Loureiro, R. J. Cava, M. Mikami, Y. Mori, M. Yoshimura, and T. Sasaki, "Coherence-incoherence and dimensional crossover in layered strongly correlated metals," *Nature*, vol. 417, no. 6889, pp. 627–630, 2002.

[25] A. A. Kordyuk, "Pseudogap from arpes experiment: Three gaps in cuprates and topological superconductivity (review article)," *Low Temperature Physics*, vol. 41, no. 5, pp. 319–341, 2015.

[26] T. J. Reber, N. C. Plumb, Y. Cao, Z. Sun, Q. Wang, K. McElroy, H. Iwasawa, M. Arita, J. S. Wen, Z. J. Xu, G. Gu, Y. Yoshida, H. Eisaki, Y. Aiura, and D. S. Dessau, "Prepairing and the "filling" gap in the cuprates from the tomographic density of states," *Physical Review B - Condensed Matter and Materials Physics*, vol. 87, no. 6, 2013.

[27] C. L. Smallwood, W. Zhang, T. L. Miller, C. Jozwiak, H. Eisaki, D.-H. Lee, and A. Lanzara, "Time- and momentum-resolved gap dynamics in $bi_2sr_2cacu_2o_{8+\delta}$," *Phys. Rev. B*, vol. 89, p. 115126, Mar 2014.

[28] F. Massee, S. D. J. Y. Huang, W. K. Siu, I. Santoso, a. Mans, a. T. Boothroyd, D. Prabhakaran, R. Follath, a. Varykhalov, L. Patthey, M. Shi, J. B. Goedkoop, and M. S. Golden, "Bilayer manganites: polarons in the midst of a metallic breakdown," *Nature Physics*, vol. 7, no. 9, p. 7, 2011.

[29] J. Kim, a. H. Said, D. Casa, M. H. Upton, T. Gog, M. Daghofer, G. Jackeli, J. van den Brink,

G. Khaliullin, and B. J. Kim, "Large Spin-Wave Energy Gap in the Bilayer Iridate $Sr_3Ir_2O_7$: Evidence for Enhanced Dipolar Interactions Near the Mott Metal-Insulator Transition," *Physical Review Letters*, vol. 109, p. 157402, oct 2012.

[30] S. Boseggia, R. Springell, H. C. Walker, A. T. Boothroyd, D. Prabhakaran, D. Wermeille, L. Bouchenoire, S. P. Collins, and D. F. McMorrow, "Antiferromagnetic order and domains in $Sr_3Ir_2O_7$ probed by x-ray resonant scattering," *Phys. Rev. B*, vol. 85, p. 184432, May 2012.

[31] C. M. Varma, "Theory of the pseudogap state of the cuprates," *Phys. Rev. B*, vol. 73, p. 155113, Apr 2006.

[32] M. Uchida, K. Ishizaka, P. Hansmann, Y. Kaneko, Y. Ishida, X. Yang, R. Kumai, A. Toschi, Y. Onose, R. Arita, K. Held, O. K. Andersen, S. Shin, and Y. Tokura, "Pseudogap of metallic layered nickelate $R_{2-x}\mathrm{sr}_x\mathrm{nio}_4$ ($r = \mathrm{Nd}, \mathrm{Eu}$) crystals measured using angle-resolved photoemission spectroscopy," *Phys. Rev. Lett.*, vol. 106, p. 027001, Jan 2011.

[33] See Supplemental Material at [URL will be inserted by publisher] for details of the doping level determination and checks on sample aging and charging.